Maneuvering Target Tracking with Colored Noise

WEN-RONG WU
DAH-CHUNG CHANG
National Chiao Tung University
Taiwan

It is known that colored noise may degrade the performance of a tracking algorithm. A common remedy is to model colored noise as an autoregressive (AR) process and apply the measurement difference method. One problem with the approach is that the AR parameters are usually unknown. In this work, we propose a new method to adaptively estimate the AR parameters. It is shown that this method is simple and practically feasible. We incorporate our method into the interacting multiple model (IMM) tracking algorithm and show that the performance is almost as good as that in the known parameters case.

Manuscript received June 10, 1994; revised May 10 and August 24, 1995.

IEEE Log No. T-AES/32/4/08000.

Authors' address: Department of Communication Engineering, National Chiao Tung University, Hsinchu, Taiwan, R.O.C.

I. INTRODUCTION

A white noise observation model is widely used in tracking problem formulation. In practice, the measurement noise may not be white. This phenomenon is due to the scintillation of the target. Typically, the bandwidth of measurement noise is on the order of several hertz [3, 12]. When the measurement frequency is much lower than the noise bandwidth, the successive samples of the noise are approximately uncorrelated, and it can be seen as white. However, in many radar systems, the measurement frequency is high enough so that the correlation cannot be ignored without degrading the tracking performance.

The conventional method that alleviates the effect of colored noise is the state augmentation approach [1]. But this may cause the covariance matrix to be ill-conditioned. Bryson [2] proposed the measurement difference approach to prevent the problem. Rogers [3] modeled the colored noise as a 1st-order AR process and applied the measurement difference approach to the α-β filter. Guu and Wei [4] extended Rogers' method in [3] to maneuvering target tracking problem using the interacting multiple model (IMM) method. Besides descrete-time approaches, some researchers also investigated the continuous-time Kalman tracker under the colored noise environment. Rogers [6] derived closed-form solutions for the tracker with exponentially correlated velocity (ECV) and exponentially correlated acceleration (ECA). Arcasoy [7] used the spectral factorization method to develop expressions of the Kalman gains for the ECV and ECA tracking problems. In aforementioned approaches, they all assumed that the autoregressive (AR) coefficients are known. However, this may not be possible in the real applications. Guu and Wei [5] then further developed a method to estimate the AR parameters. Unfortunately, this method is computationally intensive and only applicable to the Makovian acceleration model. It cannot be used in some advanced tracking algorithms such as IMM.

We propose a new method to estimate the AR parameters. We first remove the state variables from measurements by passing them into a moving average (MA) filter and this results in an autoregressive moving average (ARMA) signal. It is found that the z-transform of the signal has two zeros on the unit circle. In order to obtain the AR coefficient from the ARMA signal, we further introduce an AR filter to cancel the zeros. The AR parameters are then calculated from the statistics of the output signal. However, when the target is maneuvering, the estimates will be biased. From theoretical analysis, we derive a closed-form solution to remove the bias. Our method can be implemented adaptively and is suitable for on-line processing. Simulations show that our method can estimate the parameters precisely. The

proposed algorithm and the measurement difference method are used in the IMM algorithm and significant improvement is obtained.

II. DECORRELATION PROCESS

In this section, we describe the decorrelation process in [3]. For simplicity, we assume that states of target motion are defined in the spherical coordinate such that the state equations can be decoupled into three independent channels. Then, the tracking filter can work independently on each channel [9]. The state equations in a particular channel can be described as follows

$$X_{k+1} = \phi X_k + G w_k \tag{1}$$

$$y_k = H X_k + \nu_k \tag{2}$$

where X_k is state vector, ϕ is state transition matrix, y_k is the measurement, w_k and ν_k are the state and the measurement noise, respectively. If the measurement frequency is high, the correlation of ν_k cannot be ignored. Rogers [3] modeled the continuous colored noise as a first-order AR process, which can be described as

$$\dot{\nu}(t) = -\lambda \nu(t) + \eta(t). \tag{3}$$

Sampling $\nu(t)$ with a period T, we obtain a difference equation which is

$$\nu_k = \alpha \nu_{k-1} + \eta_k \tag{4}$$

where $\alpha = e^{-\lambda T}$ and η_k is zero-mean white Gaussian noise with variance σ_η^2. To decorrelate the measurement noise, a new measurement $\overline{y}_k$, called "artificial measurement," is generated

$$\begin{aligned} \overline{y}_k &\triangleq y_k - \alpha y_{k-1} \\ &= H(x_k - \alpha x_{k-1}) + (\nu_k - \alpha \nu_{k-1}) \\ &= \overline{H} x_k + \overline{\eta}_k \end{aligned} \tag{5}$$

where

$$\overline{H} = H(I - \alpha \phi^{-1}) \tag{6}$$

$$\overline{\eta}_k = \alpha \phi^{-1} G w_{k-1} + \eta_k. \tag{7}$$

In practical applications, the first term of right-hand side in (7) is usually small and can be neglected. So, we have

$$\overline{\eta}_k \approx \eta_k. \tag{8}$$

Thus, $\overline{\eta}_k$ can be treated as white. Now, the new measurement equation (5) and the original state equation (1) can be used in the Kalman filtering.

III. ESTIMATION OF AR PARAMETERS

In the previous section, we see that if the AR parameters (α and σ_η) are known, the colored noise can be decorrelated. However, it is difficult to know the parameters in the real application. Here, we propose a method that can effectively estimate the parameters. For the ease of description, we assume that the measurement is the position of the target. Let $X_k = [x_k, v_k, a_k]^T$ where x_k, v_k, and a_k are position, velocity, and acceleration of the target, respectively, we then have the measurement equation

$$y_k = x_k + \nu_k. \tag{9}$$

Since measurements contain state variable x_k, the direct estimation of AR parameters is difficult. It will be very helpful if we can remove state variable x_k. From the Newton's law, we have

$$x_{k+1} = x_k + v_k T + \tfrac{1}{2} a_k T^2 \tag{10}$$

We now use the following operation to obtain a new signal $\overline{u}_k$ that does not involve x_k

$$\begin{aligned} \overline{u}_k &= y_k - 2y_{k-1} + y_{k-2} = (y_k - y_{k-1}) - (y_{k-1} - y_{k-2}) \\ &= (\nu_k - 2\nu_{k-1} + \nu_{k-2}) + (x_k - x_{k-1}) - (x_{k-1} - x_{k-2}) \\ &= (\nu_k - 2\nu_{k-1} + \nu_{k-2}) + (v_{k-1} - v_{k-2})T \\ &\quad + \tfrac{1}{2} a_{k-1} T^2 - \tfrac{1}{2} a_{k-2} T^2 \\ &= (\nu_k - 2\nu_{k-1} + \nu_{k-2}) + \tfrac{1}{2}(a_{k-1} + a_{k-2}) T^2. \end{aligned} \tag{11}$$

A close look reveals that the operation is essentially a MA filtering and it can completely null a linear function ($a_k = 0$). When the measurement frequency is high, the measurement (without noise) is approximately linear in a short period of time (in our case, two Ts). Thus, this simple filtering operation enables us to extract the measurement noise with little distortion. To investigate the effect of the filtering, we go to the transform domain. Taking the z-transform of (11), we have

$$\begin{aligned} \overline{u}(z) &= (1 - 2z^{-1} + z^{-2}) \nu(z) + m(z) \\ &= (1 - z^{-1})^2 \nu(z) + m(z) \end{aligned} \tag{12}$$

where

$$m(z) = \tfrac{1}{2}(z^{-1} + z^{-2}) a(z) T^2. \tag{13}$$

Note that ν_k is an AR process. From (4), we find its transfer function is

$$\nu(z) = \frac{1}{1 - \alpha z^{-1}} \eta(z). \tag{14}$$

Thus, we can represent $\overline{u}(z)$ as

$$\overline{u}(z) = \frac{(1 - z^{-1})^2}{1 - \alpha z^{-1}} \eta(z) + m(z). \tag{15}$$

When the target is nonmaneuvering, the acceleration is zero and $m(z)$ is zero. From (15), we know $\overline{u}_k$ is an ARMA process. Since there are two zeros on the unit circle, it is difficult to use the general system

identification methods to estimate the AR coefficients. To overcome this problem, we further introduce a filter to cancel the zeros. Consider the filter described by its transfer function as follows

$$F(z) = \frac{1}{(1-\rho z^{-1})^2} \tag{16}$$

where $0 \le \rho \le 1$. Passing $\bar{u}(z)$ through $F(z)$, we obtain the output (denoted as $u(z)$)

$$u(z) = \frac{(1-z^{-1})^2}{(1-\rho z^{-1})^2}\bar{u}(z) \tag{17}$$

$$= \frac{1}{1-\alpha z^{-1}}\frac{(1-z^{-1})^2}{(1-\rho z^{-1})^2}\eta(z) + \frac{m(z)}{(1-\rho z^{-1})^2}. \tag{18}$$

For nonmaneuvering cases, the second term of the right-hand side in (18) is zero. If we let $\rho = 1$, zeros are completely canceled. From (18), we see that u_k is just the colored noise ν_k, i.e.,

$$u_k = \alpha u_{k-1} + \eta_k. \tag{19}$$

Denote the autocorrelation function of u_k as $r(\cdot)$. The α can then be estimated by

$$\hat{\alpha} = \frac{\hat{r}(1)}{\hat{r}(0)}. \tag{20}$$

Here, we use an adaptive method to estimate the autocorrelation function. By the fading memory technique [15], we have

$$\hat{r}_k(0) = \beta\hat{r}_{k-1}(0) + (1-\beta)u_k^2 \tag{21}$$

$$\hat{r}_k(1) = \beta\hat{r}_{k-1}(1) + (1-\beta)u_k u_{k-1} \tag{22}$$

where $0 < \beta < 1$ is the forgetting factor. If β is large, the convergence of $\hat{r}(\cdot)$ is slow and it cannot response to the change of α quickly. The advantage of using large β is the small estimation variance. On the contrary, small β will let $\hat{r}(\cdot)$ converge fast and response quickly. However, the estimation variance is large.

When the target is maneuvering, $m(z)$ is not negligible. In this case, we cannot choose ρ as one, otherwise the low frequency components of $m(z)$ will be greatly amplified. It is easy to see this from the Fourier transform of $F(z)$

$$|F(e^{j\omega})| = \left|\frac{1}{1-\rho e^{-j\omega}}\right|^2 = \frac{1}{(1+\rho^2)-2\rho\cos\omega}. \tag{23}$$

The magnitude in (23) will become huge if $\rho = 1$ and ω is small (infinite for $\omega = 0$). This will breakdown the whole algorithm. Therefore, ρ cannot be one. From experience, we find that if ρ is 0.9 or less, the amplification effect is small compared with the first term of (18). With suitable choice of ρ, we can then

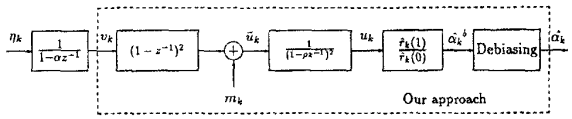

Fig. 1. Algorithm of estimating AR coefficient of colored noise.

ignore $m(z)$. Thus,

$$u(z) \approx \frac{1}{1-\alpha z^{-1}}\frac{(1-z^{-1})^2}{(1-\rho z^{-1})^2}\eta(z). \tag{24}$$

However, the nonunity ρ raises another problem. From (24), it is clear that u_k is no longer equal to ν_k and

$$\alpha \ne \frac{r(1)}{r(0)}. \tag{25}$$

The estimate of (20) is then biased. To correct the bias, we explore the relation of α and $r(1)/r(0)$. Equation (24) can be rewritten as

$$[1-(2\rho+\alpha)z^{-1} + (2\alpha\rho+\rho^2)z^{-2} - \alpha\rho^2 z^{-3}]u(z) = (1-2z^{-1}+z^{-2})\eta(z). \tag{26}$$

Thus, $u(z)$ is an ARMA process. Using the Yule–Walker equations [15], we can solve for its coefficients in terms of its autocorrelation function. Let

$$\alpha^b = \frac{r(1)}{r(0)} \tag{27}$$

$$\xi_3 = (\rho+1)^3 \tag{28}$$

$$\xi_2 = (-2\rho^2 - 10\rho - 4) + (-6\rho - 2)\alpha^b \tag{29}$$

$$\xi_1 = (-\rho^3 - 3\rho^2 + 5\rho + 7) + (8\rho + 8)\alpha^b \tag{30}$$

$$\xi_0 = (2\rho^2 + 2\rho - 4) + (-2\rho - 6)\alpha^b. \tag{31}$$

Then, α and σ_n^2 can be found as follows. We leave derivation details in Appendix A

$$\alpha = \frac{-(\xi_3+\xi_2) - \sqrt{(\xi_3+\xi_2)^2 - 4\xi_3(\xi_3+\xi_2+\xi_1)}}{2\xi_3} \tag{32}$$

and

$$\sigma_\eta^2 = -\frac{[-2\rho^3\alpha^2 + (1-\rho^4)\alpha + 2\rho]r(0) + [(\rho^2+\rho^4)\alpha^2 + (2\rho^3 - 2\rho)\alpha - (\rho^2+1)]r(1)}{(1+\rho^2)\alpha + (2\rho - 4)}. \tag{33}$$

Substituting α^b with its estimate $\hat{\alpha}_k^b$, we can obtain $\hat{\alpha}_k$ and $\hat{\sigma}_{\eta,k}^2$. The block diagram of our proposed algorithm is shown in Fig. 1.

In this paragraph, we estimate the computational requirement of our algorithm. Since the computational complexity of a multiplication/division is much higher than that of an addition/subtraction, we then ignore the operations of addition and subtraction in our complexity estimate. From Fig. 1, we know that

there are three stages in our algorithm. First, we use (17) to extract colored noise. Second, we use (21), (22), and (27) to calculate α^b. Finally, we use (28)–(33) to estimate α and σ_η^2. Totally, we need 26 multiplications, two divisions, and one square root operation for one cycle. It is shown that [13] a Kalman filter with scalar observations requires $4n^3 + 2.5n^2 + 3.5n + 3$ multiplications where n is the state dimension. The mixing operations in an IMM algorithm require $\sum_{i=1}^{m}(2n_i^2 + 2n_i + 4)$ multiplications and m exponential operations where m is the number of models and n_i is the dimension of the ith model. For example, if we use two models in the IMM algorithm; one is 2-dimensional and the other one is 3-dimensional, a complete IMM algorithm will require 240 multiplications and two exponential operations. The computational complexities of the square root, division, and exponential operations are much higher than multiplications. It is difficult to have a precise evaluation. Roughly, we can say that the computational complexity of our algorithm is approximately one-tenth of the IMM algorithm.

Though Guu and Wei [5] also used the measurement difference method to decorrelate colored noise, their AR identification algorithm is different from ours. They assumed that the acceleration of the target, a_k, is a first-order Markov process (AR process), i.e.,

$$a_{k+1} = \tau a_k + \epsilon_k \tag{34}$$

where ϵ_k is a white Gaussian process, $\sigma_\epsilon^2 = E\{\epsilon_k^2\}$ is unknown, and τ is assumed to be known. They define the innovation of the artificial measurement $\bar{y}_k$ as $\psi_k = \bar{y}_k - \tilde{y}_k$; $\tilde{y}_k$ is the prediction of $\bar{y}_k$. Using the correlation functions of ψ_k, $\varrho_j = E\{\psi_k \psi_{k-j}\}$, $j = 0,1,\ldots$, Guu and Wei derived the following relationship

$$\varrho_j = f_j \sigma_\epsilon^2 + g_j(\alpha)\sigma_\eta^2, \qquad j = 0,1,\ldots \tag{35}$$

where f_j is a scalar and $g_j(\cdot)$ is a nonlinear function of α. To solve (35), a nonlinear algorithm was used to minimize a least-squares criterion

$$\min_{\alpha,\sigma_\eta^2,\sigma_\epsilon^2} \sum_j [\hat{\varrho}_j - (f_j\sigma_\epsilon^2 + g_j(\alpha)\sigma_\eta^2)]^2 \tag{36}$$

where $\hat{\varrho}_j$ is an estimate of ϱ_j based on the innovation sequence. The problem of this approach is that many matrix and vector operations are required to obtain f_j and $g_j(\cdot)$; it is computationally intensive. In addition, the nonlinear minimization algorithm may converge to a local minimum.

IV. SIMULATION RESULTS

In this section, we carry out some simulations to demonstrate the effect of the proposed algorithm. For simplicity, we only consider a one-dimensional range tracker herein. The IMM is applied as the tracking algorithm, which is implemented by using a second-order model for the nonmaneuvering mode and two third-order models for the maneuvering mode, one is with process noise and the other is without process noise. They are described in the following equations.

1) *Nonmaneuvering mode*:

$$\begin{bmatrix} x \\ v \end{bmatrix}_{k+1} = \begin{bmatrix} 1 & T \\ 0 & 1 \end{bmatrix} \begin{bmatrix} x \\ v \end{bmatrix}_k + \begin{bmatrix} \frac{1}{2}T^2 \\ T \end{bmatrix} w_k \tag{37}$$

2) *Maneuvering mode*:

$$\begin{bmatrix} x \\ v \\ a \end{bmatrix}_{k+1} = \begin{bmatrix} 1 & T & \frac{1}{2}T^2 \\ 0 & 1 & T \\ 0 & 0 & 1 \end{bmatrix} \begin{bmatrix} x \\ v \\ a \end{bmatrix}_k + \begin{bmatrix} \frac{1}{6}T^3 \\ \frac{1}{2}T^2 \\ T \end{bmatrix} w_k^m \tag{38}$$

where w_k and w_k^m are white noises. The measurement equation is

$$y_k = x_k + \nu_k. \tag{39}$$

The Markovian transition probability matrix in IMM is chosen as

$$[p_{ij}] = \begin{bmatrix} 0.99 & 0.01 & 0.00 \\ 0.33 & 0.34 & 0.33 \\ 0.00 & 0.01 & 0.99 \end{bmatrix}. \tag{40}$$

In this simulation, the sampling period is taken as 0.05 s. The total tracking interval is 60 s. In other words, there are 1200 measurement samples. The maneuvering occurs on 20th s to 40th s with constant acceleration 40 m/s^2 (about 4g). The state noise variances are $E[w_k w_k] = 10^{-3}$ (m/s^2)^2 for the nonmaneuvering mode and $E[w_k^m w_k^m] = 0$ (m/s^2)^2, 800^2 (m/s^2)^2 for the maneuvering mode. We assume that the standard deviation of measurement noise is $\sigma_\nu = 100$ m. Two λs are used in the simulations. One is 4 s^{-1} and the other is 10 s^{-1}. The corresponding α values are 0.8187 and 0.6067, respectively. The simulation setup is the same as that in [4]. 100 Monte Carlo runs are carried out and the average results are shown under the root mean square error (RMSE) criterion

$$\text{RMSE}(k) = \sqrt{\frac{1}{m}\sum_{i=1}^{m}(x_k - \hat{x}_k^i)^2}$$
$$k = 1,2,\ldots,1200; \quad m = 100 \tag{41}$$

where $\hat{x}_k^i$ denotes state estimate of the ith Monte Carlo run for the kth sample.

We first examine the behaviors of the roots in (32). Fig. 2 shows the plot of α versus α^b for different ρ values. Note that not all α^b is legitimate. The value inside the square root in (32) must be greater than or equal to zero. From Fig. 2, we see that if ρ approximates to one, the corresponding curve will be

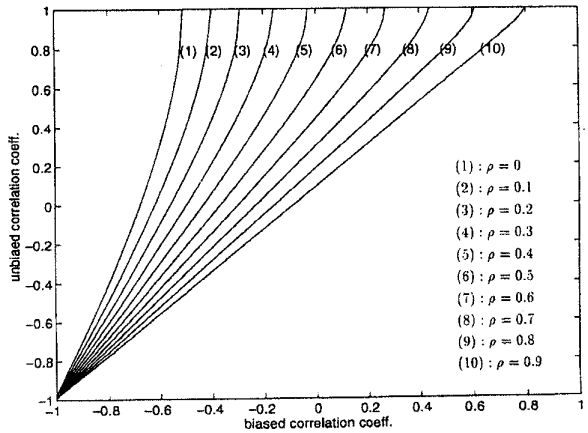

Fig. 2. Behavior of correct root for different ρ.

completely linear with unit slope. This implies that the estimator in (20) yields unbiased estimates. If $\rho \neq 1$, the estimate is biased. Also note that for smaller ρ the slope of the curve is larger. This indicates that the resolution for α^b is poorer. This will adversely affect the α estimate. All the curves in Fig. 2 are above the line $\alpha = \alpha^b$ and pass through $(-1,-1)$. In addition, their slopes are increasing. Thus, we can say that the larger the α is, the more bias α will have. For $\alpha = -1$, there is almost no bias.

To further study the effect of ρ, we plot the estimates for the whole tracking interval. Here, we assume that $\alpha = 0.8187$ for whole interval. Figs. 3 and 4 show the results of α_k and $\sigma_{\eta,k}$ estimates for different ρ values. The β is taken as 0.99. Generally, we find that larger ρ will have better results. However, too large ρ will amplify the m_k term in (18) when target is maneuvering. This results in poorer results. For $\rho = 0.9$, we see that the estimates are almost not affected by maneuvering. In the case, the estimate error of α and σ_η is around 0.075 and 4, which is quite small ($\sigma_\eta = 57.4$). We also simulated another case that $\alpha = 0.6067$. The results are similar to those obtained previously and is therefore not shown. One

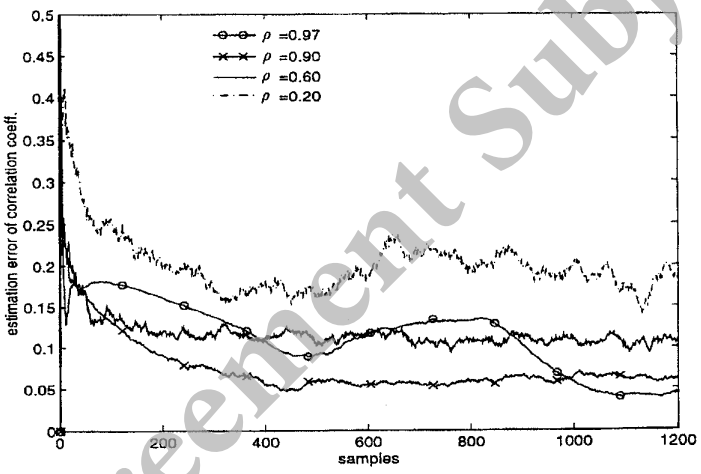

Fig. 3. Relation of α estimation error and ρ ($\alpha = 0.8187$, $\beta = 0.99$).

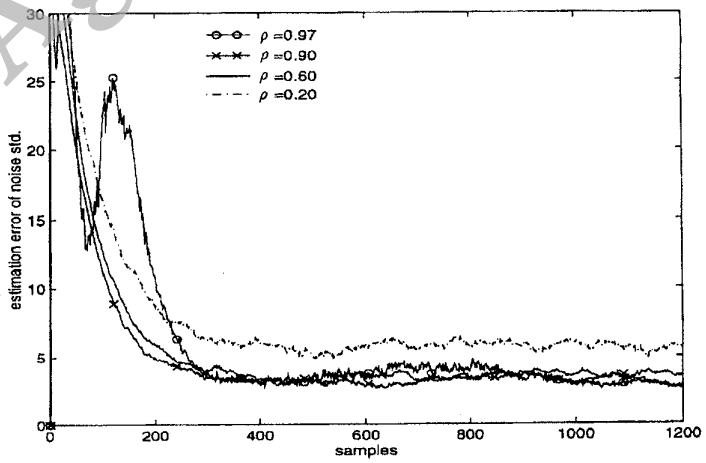

Fig. 4. Relation of σ_η estimation error and ρ ($\sigma_\nu = 100$, $\beta = 0.99$).

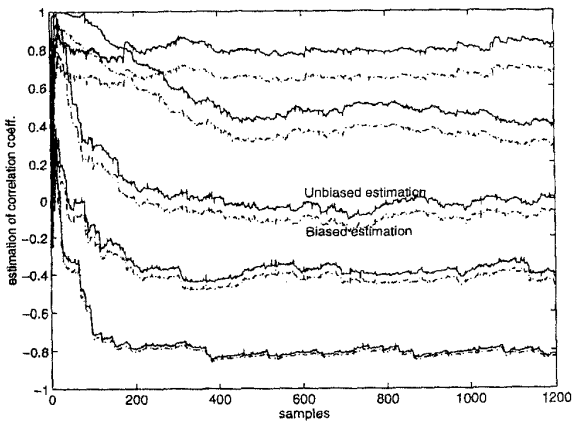

Fig. 5. Unbiased and biased estimations of $\alpha = 0.8, 0.4, 0, -0.4,$ and -0.8 ($\rho = 0.9$).

thing different is that for $\rho = 0.97$, the amplification of m_k is more serious than that in $\alpha = 0.8187$. However, for $\rho = 0.9$, the estimate is almost not affected.

In Fig. 5, we show the simulation result (single realization) for the estimation of α with and without bias. Five α values are used. They are 0.8, 0.4, 0, -0.4, and -0.8. We set $\rho = 0.9$ and $\beta = 0.995$. It is clear that for smaller α, the bias is smaller. This agrees with our induction from Fig. 2.

As aforementioned, α_k is adaptively estimated and the convergence rate depends on the β value. Smaller β has better tracking property but the estimation error is larger. To investigate the tracking property, we now let $\alpha_k = 0.8187$ for nonmaneuvering period and $\alpha_k = 0.6067$ for maneuvering period. Note that α_k experiences abrupt changes during the tracking period. Figs. 6 and 7 show the performance of estimates of α_k and $\sigma_{\eta,k}$ for different β values. Here, we set $\rho = 0.9$. In this experiment, we initiate the tracker 40 s before the formal tracking period. The purpose is to investigate the steady state behavior of our algorithm. From the figures, we verify the statement made

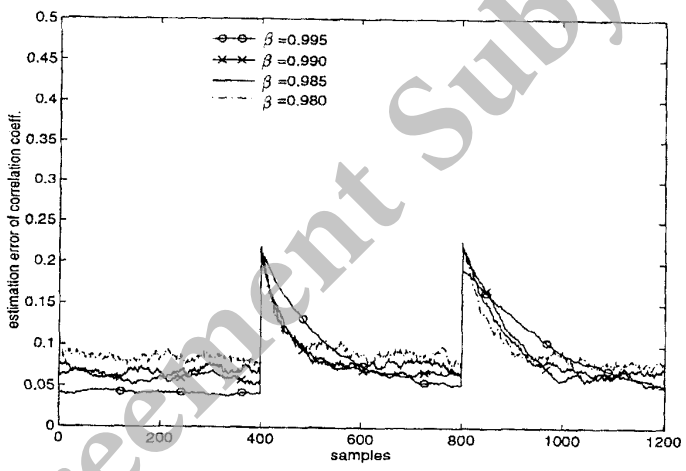

Fig. 6. Relation of α estimation error and β ($\rho = 0.9$).

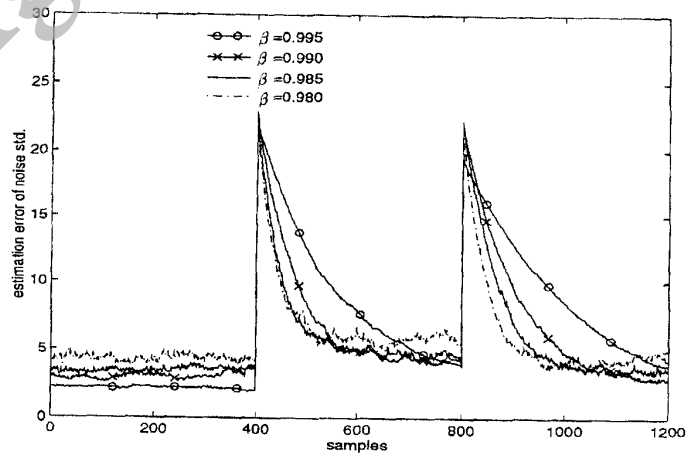

Fig. 7. Relation of σ_η estimation error and β ($\rho = 0.9$).

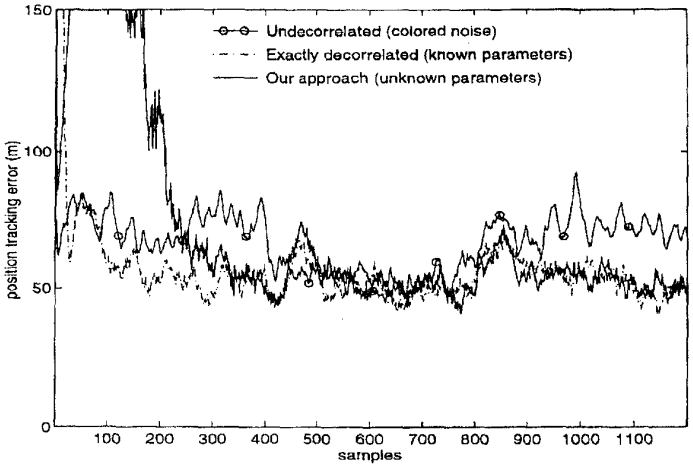

Fig. 8. Performance of position tracking in colored noise ($\rho = 0.9$, $\beta = 0.99$).

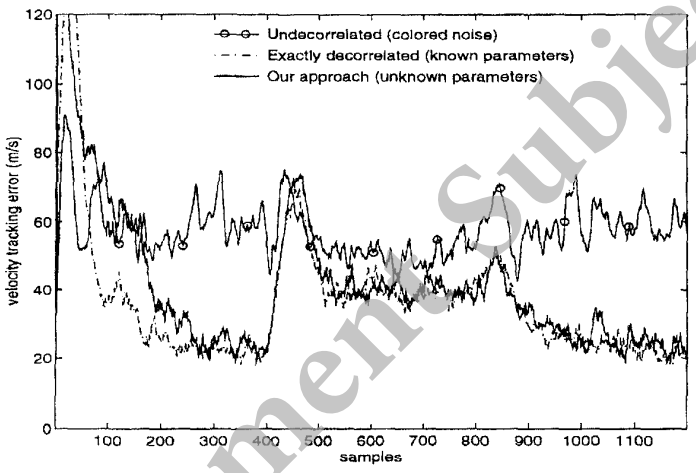

Fig. 9. Performance of velocity tracking in colored noise ($\rho = 0.9$, $\beta = 0.99$).

before. For $\beta = 0.99$, we find that it provides a good compromise between convergence rate and estimation error.

From the above result, we know that ρ should be used as large as possible. The main factor limit ρ is m_k. From (13), we find m_k is determined by target acceleration a_k and sampling period T. If T is smaller, large ρ can be used. Thus, we can conclude that the higher the measurement frequency is, the better our algorithm will work. β determines the tracking property and should be chosen according to how fast α will change. For slow changing α, β can be large. It seems that negative α is easier to work with (small bias). This can be explained by the fact that the position measurement is a low-pass signal while the colored noise is a high-pass signal (for negative α). Thus, it is easier to filter out the noise.

Finally, our approach is applied to the maneuvering target tracking with colored noise. In Figs. 8–10, we show the tracking performances for cases without decorrelation, with exact decorrelation (given the AR parameters), and with the proposed decorrelation scheme. We assume $\alpha_k = 0.8187$ for target nonmaneuvering period and $\alpha_k = 0.6067$ for maneuvering period. The rest of the parameters are chosen as $\rho = 0.9$ and $\beta = 0.99$. This choice can make the estimation of α and σ_n insensitive to maneuvering and abrupt changes of parameters. From these figures, we can clearly see that the performance of the decorrelated scheme is considerably better than that of undecorrelated one, specially in the velocity and acceleration estimates. The performance of the proposed algorithm is almost as good as that in the known parameters case. The structure of the proposed algorithm is simple and practically feasible. Also, it can adaptively track the variation of the AR parameters. This makes our algorithm is suitable for real-time applications.

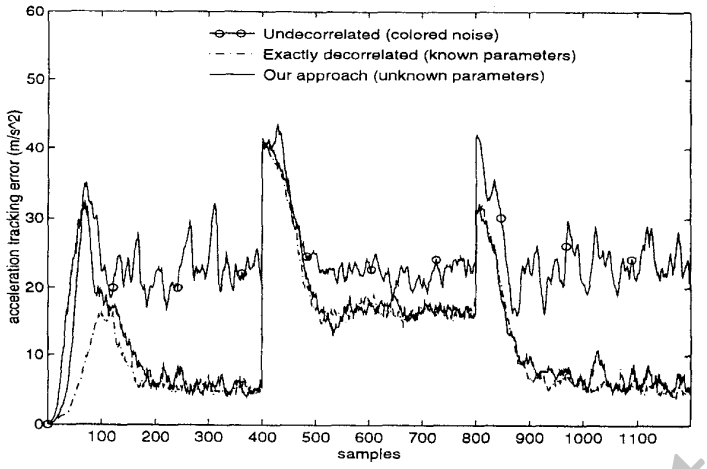

Fig. 10. Performance of acceleration tracking in colored noise ($\rho = 0.9$, $\beta = 0.99$).

V. CONCLUSION

We have proposed a new algorithm to identify the parameters of colored noise, which can be applied to maneuvering target tracking. Our algorithm is different from that of Guu and Wei [5]. We do not need the assumption of Markovian acceleration for the maneuvering target. Thus, the IMM algorithm can be used to achieve better tracking performance. From simulations, we find that our algorithm identifies the parameters properly such that the tracking performance is almost as good as that in the known parameters case. The simple structure of the algorithm makes it easy to be implemented. In (2), we assume that the only noise component is colored noise ν_k which is modeled as a first-order AR process. If other kind of noise such as white noise also exists, the mixed noise will not be an AR process any more. It can be shown that an AR process plus a white process is an ARMA process [14]. In this case, our algorithm becomes a suboptimal approach.

APPENDIX A

The Yule–Walker equations of (26) are

$$r(0) - a_1 r(1) - a_2 r(2) - a_3 r(3) = (a_1^2 - 4a_1 + a_2 + 6)\sigma_\eta^2 \tag{42}$$

$$-a_1 r(0) + (1 - a_2) r(1) - a_3 r(2) = (a_1 - 4)\sigma_\eta^2 \tag{43}$$

$$-a_2 r(0) - (a_1 + a_3) r(1) + r(2) = \sigma_\eta^2 \tag{44}$$

$$-a_3 r(0) - a_2 r(1) - a_1 r(2) + r(3) = 0 \tag{45}$$

where

$$a_1 = 2\rho + \alpha \tag{46}$$

$$a_2 = -(2\rho\alpha + \rho^2) \tag{47}$$

$$a_3 = \rho^2 \alpha. \tag{48}$$

Substituting $r(2)$ and $r(3)$ in (42) and (43) by using (44) and (45), we have

$$\begin{aligned}(a_2^2 + a_1 a_2 a_3 + a_3^2 - 1) r(0) \\ + (a_1 + a_1 a_2 + 2a_2 a_3 + a_1^2 a_3 + a_1 a_3^2) r(1) \\ + (a_1^2 - 4a_1 + 2a_2 + a_1 a_3 + 6)\sigma_\eta^2 = 0\end{aligned} \tag{49}$$

and

$$\begin{aligned}(a_1 + a_2 a_3) r(0) + (a_2 + a_1 a_3 + a_3^2 - 1) r(1) \\ + (a_1 + a_3 - 4)\sigma_\eta^2 = 0.\end{aligned} \tag{50}$$

From (46)–(50), we have

$$\begin{aligned}&[-2\rho^3\alpha^3 + (4\rho^2 - 4\rho^4)\alpha^2 + (4\rho^3 - 2\rho^5)\alpha + \rho^4 - 1] r(0) \\ &\quad + [(\rho^2 + \rho^4)\alpha^3 + (2\rho^5 - 2\rho)\alpha^2 \\ &\quad\quad + (2\rho^4 - 5\rho^2 + 1)\alpha + (2\rho - 2\rho^3)] r(1) \\ &\quad + [(1 + \rho^2)\alpha^2 + (2\rho^3 - 4)\alpha \\ &\quad\quad + (2\rho^2 - 8\rho + 6)]\sigma_\eta^2 = 0\end{aligned} \tag{51}$$

and

$$\begin{aligned}&[-2\rho^3\alpha^2 + (1 - \rho^4)\alpha + 2\rho] r(0) \\ &\quad + [(\rho^2 + \rho^4)\alpha^2 + (2\rho^3 - 2\rho)\alpha - (\rho^2 + 1)] r(1) \\ &\quad + [(1 + \rho^2)\alpha + (2\rho - 4)]\sigma_\eta^2 = 0.\end{aligned} \tag{52}$$

From (52), we yield

$$\sigma_\eta^2 = -\frac{[-2\rho^3\alpha^2 + (1 - \rho^4)\alpha + 2\rho] r(0) + [(\rho^2 + \rho^4)\alpha^2 + (2\rho^3 - 2\rho)\alpha - (\rho^2 + 1)] r(1)}{(1 + \rho^2)\alpha + (2\rho - 4)}. \tag{53}$$

Replacing σ_η^2 in (51) by (53) and simplifying the equation, we have

$$\xi_3\alpha^3 + \xi_2\alpha^2 + \xi_1\alpha + \xi_0 = 0 \tag{54}$$

where

$$\xi_3 = (\rho + 1)^3 \tag{55}$$

$$\xi_2 = (-2\rho^2 - 10\rho - 4) + (-6\rho - 2)\alpha^b \tag{56}$$

$$\xi_1 = (-\rho^3 - 3\rho^2 + 5\rho + 7) + (8\rho + 8)\alpha^b \tag{57}$$

$$\xi_0 = (2\rho^2 + 2\rho - 4) + (-2\rho - 6)\alpha^b. \tag{58}$$

Note that $\xi_3 + \xi_2 + \xi_1 + \xi_0 = 0$. It implies that $\alpha = 1$ is one root of (54). But we know $\alpha \neq 1$ and this root can be discarded. So, (54) is simplified as

$$\xi_3\alpha^2 + (\xi_3 + \xi_2)\alpha + (\xi_3 + \xi_2 + \xi_1) = 0. \tag{59}$$

There are two roots in (59). They are

$$\alpha = \begin{cases} \dfrac{-(\xi_3 + \xi_2) + \sqrt{(\xi_3 + \xi_2)^2 - 4\xi_3(\xi_3 + \xi_2 + \xi_1)}}{2\xi_3} \\ \dfrac{-(\xi_3 + \xi_2) - \sqrt{(\xi_3 + \xi_2)^2 - 4\xi_3(\xi_3 + \xi_2 + \xi_1)}}{2\xi_3} \end{cases}. \tag{60}$$

From numerical evaluation, we find out that the first root in (60) is greater than one for $0 \leq \rho < 1$. Thus the second root is the correct solution.

REFERENCES

[1] Kalman, R. E. (1963)
New method in Wiener filtering theory.
In J. L. Bogdanoff and F. Kozin (Eds.), *Proceedings of the First Symposium on Engineering Applications of Random Function Theory and Probability*.
New York: Wiley, 1963, 270–388.

[2] Bryson, A. E., and Henrikson, L. J. (1968)
Estimation using sampled data containing sequentially correlated noise.
Journal of Spacecraft, **5**, 6 (1968), 662–665.

[3] Rogers, S. R. (1987)
Alpha-beta filter with correlated measurement noise.
IEEE Transactions on Aerospace and Electronic Systems, **AES-23**, 4 (1987), 592–594.

[4] Guu, J. A., and Wei, C. H. (1991)
Maneuvering target tracking using IMM method at high measurement frequency.
IEEE Transactions on Aerospace and Electronic Systems, **27**, 3 (1991), 514–519.

[5] Guu, J. A., and Wei, C. H. (1991)
Tracking technique for maneuvering target with correlated measurement noise and unknown parameters.
IEE Proceedings, Pt. F, **138**, 3 (June 1991), 278–288.

[6] Rogers, S. R. (1990)
Continuous-time ECV and ECA track filters with colored measurement noise.
IEEE Transactions on Aerospace and Electronic Systems, **26** (1990), 663–666.

[7] Arcasoy, C. C., and Koc, B. (1994)
Analytical solution for continuous-time Kalman tracking filters with colored measurement noise in frequency domain.
IEEE Transactions on Aerospace and Electronic Systems, **30** (1994), 1059–1063.

[8] Singer, R. A. (1970)
Estimating optimal tracking filter performance for manned maneuvering target tracking.
IEEE Transactions on Aerospace and Electronic Systems, **AES-6**, 4 (1970), 473–483.

[9] Gholson, N. H., and Moose, R. L. (1977)
Maneuvering target tracking using adaptive state estimation.
IEEE Transactions on Aerospace and Electronic Systems, **AES-15** (May 1977), 448–456.

[10] Blom, H. A. P., and Bar-Shalom, Y. (1988)
The interacting multiple model algorithm for systems with Makovian switching coefficients.
IEEE Transactions on Automatic Control, **33** (Aug. 1988), 780–783.

[11] Bar-Shalom, Y., Chang, K. C., and Blom, H. A. P. (1989)
Tracking a maneuvering target using input estimation versus the interacting multiple model algorithm.
IEEE Transactions on Aerospace and Electronic Systems, **25** (Mar. 1989), 296–300.

[12] Skolnik, M. I. (1990)
Radar Handbook.
New York: McGraw-Hill, 1990.

[13] Grewal, M. S., and Andrews, A. P. (1993)
Kalman Filtering: Theory and Practice.
New York: Prentice-Hall, 1993.

[14] Pagano, M. (1974)
Estimation of models of autoregressive signal plus white noise.
Annals of Mathematical Statistics (1974), 99–108.

[15] Haykin, S. (1991)
Adaptive Filter Theory.
Englewood Cliffs, NJ: Prentice-Hall, 1991.

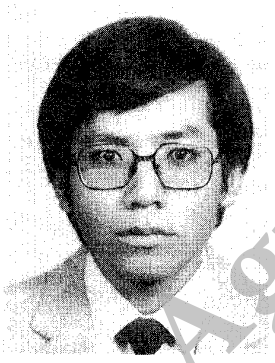

Wen-Rong Wu was born in Taiwan, R.O.C., in 1958. He received his B.S. degree in mechanical engineering from Tatung Institute of Technology, Taiwan, in 1980, M.S. degrees in mechanical and electrical engineering, and Ph.D. degree in electrical engineering from State University of New York at Buffalo in 1985, 1986, and 1989, respectively.

Since August 1988, he has been a faculty member in the Department of Communication Engineering in National Chiao Tung University, Taiwan. His research interests include estimation theory, digital signal processing, and image processing.

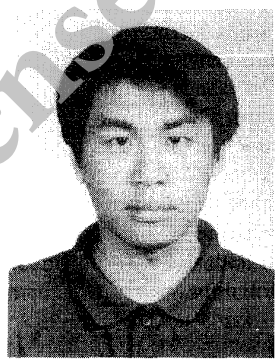

Dah-Chung Chang was born in Chia-Yi, Taiwan on June 13, 1969. He received the B.S. degree in electronic engineering from the Fu-Jen Catholic University, Taipei, Taiwan, in 1991 and the M.S. degree in electrical engineering from the National Chiao Tung University (NCTU), Hsinchu, Taiwan, in 1993.

He is currently with the image laboratory in the Department of Communication Engineering at NCTU and working toward the Ph.D. degree. His study interests include the area of detection and estimation theory, digital communications, signal processing, and radar tracking.